Publishing House
AKAPIT

COMPUTER METHODS IN MATERIALS SCIENCE

Informatyka w Technologii Materiałów

Vol. 7, 2007, No. 1

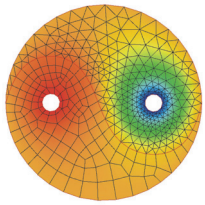

CREEP-FATIGUE OF MULTI-PART CONTAINER DURING HOT EXTRUSION OF COPPER - SIMULATION AND EXPERIMENTAL COMPARISON

FRIEDRICH KRUMPHALS[1], THOMAS WLANIS[1], CHRISTOF SOMMITSCH[1,2], CHRISTIAN REDL[3]

[1] Christian Doppler Laboratory For Materials Modelling And Simulation, University of Leoben, Franz-Josef-Strasse 18, 8700, Leoben, Austria
[2] Chair of Metal Forming, University of Leoben, Franz-Josef-Strasse 18, 8700, Leoben, Austria
[3] Böhler Edelstahl GmbH, Mariazellerstrasse 25, 8605, Kapfenberg, Austria

Abstract

The present paper shows the development of temperatures, stresses and lifetime consumption during three copper extrusion cycles in a two-part container. The simulation of the heat treatment and the resulting state of the container used was the basis for the subsequent modelling of the cyclic loads during the press cycles. The numerical FEM extrusion simulation consists of the plastic simulation of the billet extrusion with rigid tools as well as of the subsequent simulation of several cycles of the same process, only considering the elastic container and using the time dependent temperature and pressure boundary conditions at the contact surface billet-liner. The reason for this procedure is the much shorter calculation time for the elastic container model with specified boundary conditions in comparison to the plastic extrusion process, especially for several extrusion cycles. Both a constitutive law and a lifetime consumption rule were coupled to the elastic container model in order to get the local inelastic strain rates and the damage rate, respectively. To verify the calculated temperature and pressure boundary conditions at the contact surface billet-liner, an experimental extruding test facility was constructed.

Key words: extrusion, hot work tool steels, creep-fatigue, lifetime, damage

1. INTRODUCTION

Extrusion tools exhibit a complex strain-time pattern under a variety of cyclic loading conditions and thus are prone to failure by creep-fatigue interactions (Wieser et al., (2004)). Elevated temperature failure by creep-fatigue processes is time dependent and often involves deformation path dependent interactions of cracks with grain boundary cavities (Majumdar and Maiya, (1980)). The extrusion industry tries to accelerate the manufacturing process by increasing the billet temperature and/or by accelerating the press speed that raise the loading of the tools. On the other side the tool steel producers develop enhanced more homogeneous and cleaner materials in order to increase tools lifetime. Finite element simulation of the extrusion process to get the temperature and stress evolution in the container, coupled with constitutive equations as well as lifetime consumption models in order to calculate both the inelastic strains and the tools lifetime, help to optimise the extrusion process and to compare the operating times of different hot work tool steels (Sommitsch et al., (2006 a, 2006 b)).

Viscoplastic constitutive models were developed in the past to take into account the inelastic behaviour of the material during creep-fatigue loads, see, e.g. Krausz and Krausz, (1996); Lemaitre and Chaboche, (1990); Chaboche, (1993). In the present study the Chaboche model was selected and cali-

ISSN 1641-8581

brated to the material response of a hot work tool steel between 470°C and 590°C. To extend the prediction capability of Chaboche's model for non-isothermal processes a temperature-rate term was added to the isotropic hardening rule (Olschewski and Sievert, (1993)). Additionally, a creep-fatigue lifetime rule for complex processes was investigated that is independent of single loading parameters, like stress or strain ranges or corresponding maxima, for the description of an entire cycle. Instead this rule evaluates the total damage in each time increment and accumulates that to the lifetime consumption.

2. MODELLING AND SIMULATION

The numerical extrusion simulation consists of the simulation of several cycles of the same process, only considering the elastic 2-part container and using the time dependent temperature and radial stress boundary conditions at the inner diameter of the liner.

2.1. Extrusion model

To predict damage, the accurate knowledge of the unsteady local thermal and mechanical loading within one cycle on the inner diameter of the liner is of particular importance. Hence the thermo-mechanical load of a container during extrusion of a billet was analysed by means of the finite element program HyperXtrude^{TM} v.8.0. Since the container assembly is symmetrical, a 2D axi-symmetric model of the container was used. The die, ram and die-holder were assumed to be rigid. The following temperature-dependent thermo-physical material properties were chosen: thermal expansion 10^{-5} [K^{-1}], thermal conductivity 360 [$Wm^{-1}K^{-1}$], specific heat 383 [J $kg^{-1}K^{-1}$] for the liner made of Böhler W400 VMR and for the mantle made of Böhler W300 ESR. The length L, inner diameter D_i and outer diameter D_o of the liner, mantle and billet, respectively, were assumed to be:
Liner: L=115 mm; D_i =45 mm, D_o=105 mm
Mantle: L=115 mm; D_i=105 mm; D_o =270 mm
Billet: L=100 mm; D=45 mm

The shrink-fitting of the mantle was simulated by a shrinkage of 0.8‰. For the billet material, electro copper was chosen with an initial temperature of 930°C. Figure 1 displays the steady state temperature (a) as well as the stress distribution (b) in the billet for copper extrusion. The maximum thermal load appears at the inner diameter of the liner near the die, where the contact time with the billet during extrusion lasts longest, however the maximum stress can be found at the contact zone ram / billet.

The simulated processes are listed below:
- shrink-fitting of the mantle (0.8‰),
- pre-heating of the container to a working temperature of 500°C,
- pressing on the container against the die-holder,
- forward extrusion of the billet with a ram speed of 7 mm/s

From the development of the radial stress at the inner diameter of the liner, the non-uniform load state of the container as well as the steady state operating condition and thus the time and axial position dependent boundary conditions for the container can be derived. These boundary conditions were used for a minimisation of calculation time, which is described in the following.

2.2. Model of cyclic container loads

For the calculation of the cyclic temperature and stress evolution in the container, Abaqus Standard^{TM} v.6.5-1 FEM calculations were conducted with elastic liner and mantle. Since the container assembly is symmetrical, an axi-symmetric model of the container was used. Figure 2 shows the von Mises stress distribution in the container after 15 extrusion cycles.

The reason of this non-uniform stress distribution is the complex load case, which consists of:
- shrinkage stresses after shrink-fitting,
- axial stresses as a result of pressing on the container against the die-holder,
- thermal stresses due to the pre-heating to working temperature and the temperature rise during an extrusion cycle,
- axial stresses and radial compressive stresses during one extrusion cycle at the contact surfacebetween billet and inner diameter of the liner.

3. SMALL SCALE EXTRUSION

For the experimental analysis of the container load and thus the model verification, a hydraulic 100t press was adapted to small scale extrusion experiments. The measuring system for the evaluation of both compressive stresses reacting at the liner and temperature distribution in the container is depicted in figures 3, 4. To obtain a pressure distribution, three holes at different levels (L1, L2, L3 in figure 4) were drilled into the container, with only a thin container wall thickness left. The pressure force is

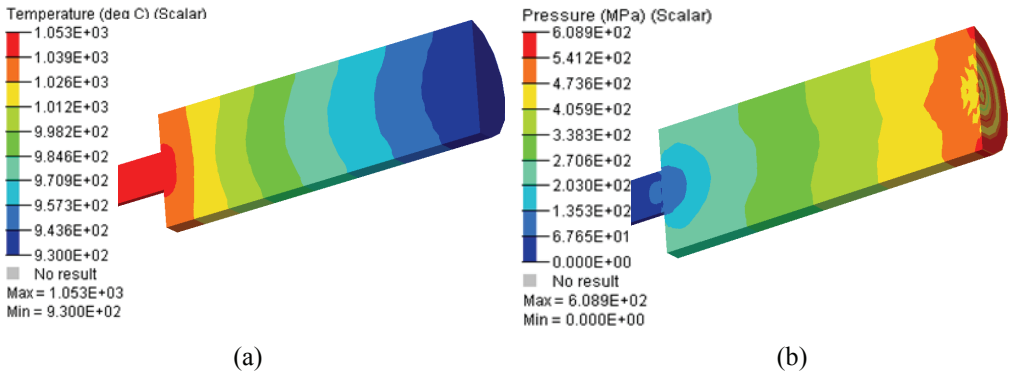

(a) (b)

Fig. 1. Steady state temperature (a) as well as stress (b) distribution in the copper billet with 930°C initial temperature.

wall against damage. The same drilled holes are also used for temperature measurements (figure 4). Measuring points are positioned near the inner wall of the liner (T1, T2, T3) and in the centre of the container (T4). Point T2 near the inner wall was used for heat control.

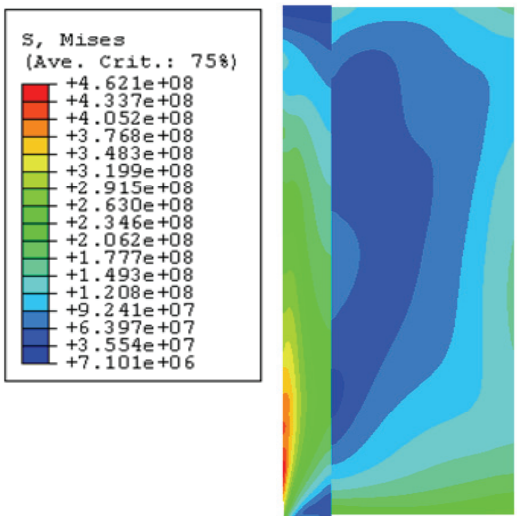

Fig. 2. Von Mises stress [Pa] distribution in the container after 15 extrusion cycles; extrusion direction top-bottom.

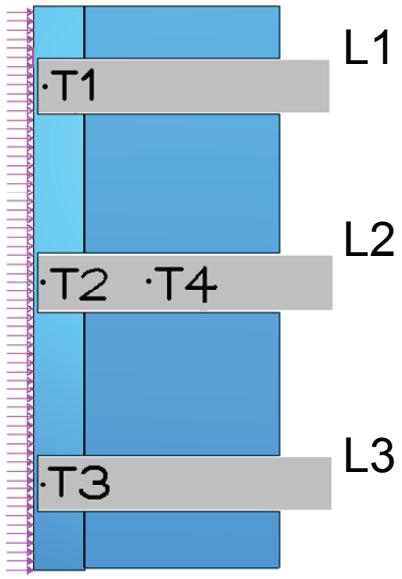

Fig. 4. Schematically drawing with the positions of temperature measuring points. The extrusion direction is top-bottom.

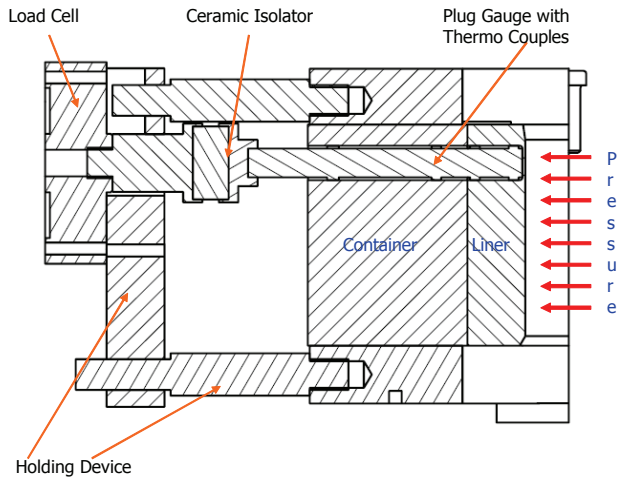

Fig. 3. Drawing of a pressure and temperature measurement system (here: top measuring point, L1).

transmitted through a plug gauge with a ceramic temperature isolator to a load cell (figure 3). The system plug gauge / load cell sustains the container

4. EXPERIMENTAL EVALUATION AND COMPARISON

The calibration of the load cells took place with a pressure test by means of hydraulic pressure. After this calibration it was possible to correlate these values, indicated by the three load cells to the real pressure loading at these vertical levels. Hence a pressure distribution, with decreasing maxima from the top to the bottom level of the container developed (figure 5a). The pressure values increase immediately from the beginning of the extrusion cycle to a constant maximum until they abruptly decrease when the ram passes their vertical level. The slightly higher values in the experiment (compare figures 1b and 5a) result from the increasing flow stress due to decreasing billet temperatures, which was not considered in the simulation.

Contrary to industrial extrusion practise, it was necessary to extrude the copper billets billet-to-billet

in laboratory scale in order to avoid several complications. Especially the remarkably high evaluated pressure peak at the beginning of the cycle occurring at the bottom level measuring point (L3 in figure 5a) resulted from a thin, about 8 to 10 mm thick billet rest with an even higher flow stress due to the cooling during the loading process. After a cycle the load cells still showed pressure values, which arose from a small plastic deformation of the thin inner liner wall in front of the plug gauges.

To evaluate thermal loads, temperature measuring points were positioned at the plug gauges (figure 4) about 5 mm behind the inner liner wall. The higher values (ca. 80K) in the simulation in comparison to the experiment resulted from the lower heat transfer between liner and plug gauge. The maximum temperature value occurred time-delayed some seconds after the extrusion cycle (figure 5b).

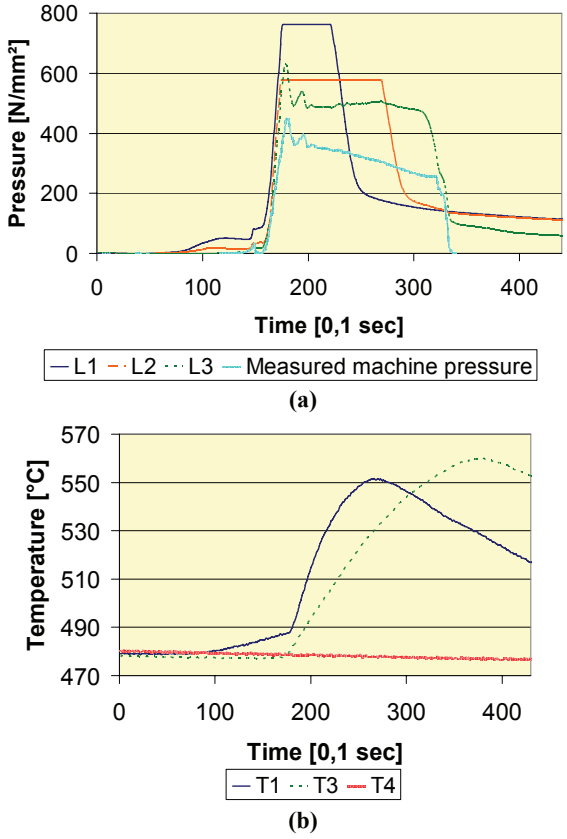

Fig. 5. *Pressure evaluation for 930°C billet and 500°C liner temperature, cycle 3 (a) and temperature evaluation for 930°C billet and 500°C liner temperature, cycle 4 (b).*

In fact the measured pressure and temperature values reflect the tendency of the simulated data very well, while the amount was not exactly conforming which could be a reason of non consistent testing parameters.

5. MODEL FOR THE DEFORMATION BEHAVIOUR

For this investigation a viscoplastic model was used according to Chaboche (1993), where the total strain $\boldsymbol{\varepsilon}$ was taken to be composed of elastic $\boldsymbol{\varepsilon}_e$, thermal $\boldsymbol{\varepsilon}_{th}$ as well as inelastic $\boldsymbol{\varepsilon}_{in}$ parts

$$\boldsymbol{\varepsilon} = \boldsymbol{\varepsilon}_e(\boldsymbol{\sigma}) + \boldsymbol{\varepsilon}_{in} + \boldsymbol{\varepsilon}_{th}(T) \quad , \quad \boldsymbol{\varepsilon}_{th}(T) = \varepsilon_{th}(T)\,\mathbf{1} \quad (1)$$

and the Hookean law was given by

$$\boldsymbol{\sigma} = 2G\,\boldsymbol{\varepsilon}_e' + \frac{E}{3(1-2\nu)}\,\mathrm{tr}\,\boldsymbol{\varepsilon}_e\,\mathbf{1}, \qquad (2)$$

with G denotes the shear modulus, E the Young's modulus, ν the Poisson's ratio and the deviator of the elastic strain tensor $\boldsymbol{\varepsilon}_e'$

$$\boldsymbol{\varepsilon}_e' := \boldsymbol{\varepsilon}_e - \tfrac{1}{3}\,\mathrm{tr}\,\boldsymbol{\varepsilon}_e\,\mathbf{1} \quad , \quad \mathrm{tr}\,\boldsymbol{\varepsilon}_e := \varepsilon_{e,1} + \varepsilon_{e,2} + \varepsilon_{e,3} \quad (3).$$

For the lifetime prediction of highly stressed extrusion tools during service, taking into account the inelastic strain rate during a cycle, it was necessary to be able to assess the inelastic stress-strain response of the material (Frenz et al., 1997). The influence of the thermo-mechanical history on the current stress-strain behaviour was described with internal (non-measurable) variables, beside the measurable (external) variables of deformation, time, temperature and stress (Lemaitre and Chaboche, 1990). The evolution equations for the internal variables were given by flow and hardening rules. In viscoplastic, i.e. unified inelastic, models, creep and plasticity were covered within a single inelastic strain variable in order to describe creep-plasticity interaction. The flow rule, i.e. the evolution equation for the inelastic strain is according to Chaboche (1993)

$$\dot{\boldsymbol{\varepsilon}}_{in} = \frac{3}{2}\left\langle \frac{J_2(\mathbf{S}-\mathbf{X}) - (k+R)}{K} \right\rangle^n \frac{\mathbf{S}-\mathbf{X}}{J_2(\mathbf{S}-\mathbf{X})}$$

$$\langle y \rangle := \begin{cases} y, \text{if } y>0 \\ 0, \text{otherwise} \end{cases}, \qquad (4)$$

specifying $\mathbf{S}$ as the applied stress deviator, k as the initial elastic limit, R as the increase of the elastic limit due to hardening, $\mathbf{X}$ as the internal back stress tensor, describing kinematic hardening and K as a material parameter. Olschewski et al. (1993) have proposed a certain type of a thermal-mechanical evolution equation for the isotropic hardening vari-

able R = Q(T) r in order to describe non-isothermal material behaviour, T denotes the temperature:

$$\dot{\mathrm{R}} = Q\,\dot{\mathrm{r}} + \frac{\mathrm{R}}{Q}\frac{\mathrm{d}Q}{\mathrm{dT}}\dot{\mathrm{T}} \qquad (5)$$

with Q as the saturation parameter of R at isothermal loading and r as the related isotropic hardening variable with the evolution equation

$$\dot{\mathrm{r}} = b\left(1-\frac{\mathrm{R}}{Q}\right)\dot{\mathrm{p}} - \frac{f}{Q}\left(\frac{\mathrm{R}}{Q}\right)^{s},$$

$$\mathrm{r(t=0)} = 0 \quad , \quad \dot{\mathrm{p}} := \sqrt{\tfrac{2}{3}}\left\|\dot{\boldsymbol{\varepsilon}}_{\mathrm{in}}\right\| \qquad (6)$$

where b, f and s are material parameters adapting the isotropic hardening and static recovering, respectively, and $\dot{\mathrm{p}}$ is the inelastic Mises equivalent strain-rate.

The rate equations for the kinematic hardening variables obey a unique format. The back stress $\mathbf{X}$ is decomposed into independent variables $\mathbf{X}_{\mathrm{i}}$, each of them being of the same rule. As shown in previous studies, two or three of such variables are sufficient to describe, very correctly, the real materials. In this work two independent variables have been chosen

$$\mathbf{X} = \mathbf{X}_1 + \mathbf{X}_2 \quad , \quad \mathbf{X}_{\mathrm{i}} = \tfrac{2}{3}\,a_{\mathrm{i}}(\mathrm{T})\,\boldsymbol{\alpha}_{\mathrm{i}} \quad , \quad \mathrm{i} = 1,2 \quad (7),$$

where a_i (T) are saturation parameters of the internal back-stresses $\mathbf{X}_{\mathrm{i}}$, and $\boldsymbol{\alpha}_{\mathrm{i}}$ are related kinematic hardening variables:

$$\dot{\boldsymbol{\alpha}}_{\mathrm{i}} = c_{\mathrm{i}}\,\dot{\boldsymbol{\varepsilon}}_{\mathrm{in}} - \frac{3}{2}\,c_{\mathrm{i}}\frac{\mathbf{X}_{\mathrm{i}}}{a_{\mathrm{i}}}\,\dot{\mathrm{p}} - \frac{3}{2}\frac{d_{\mathrm{i}}}{a_{\mathrm{i}}}\left(\frac{\mathrm{J}_2(\mathbf{X}_{\mathrm{i}})}{a_{\mathrm{i}}}\right)^{m_{\mathrm{i}}}\frac{\mathbf{X}_{\mathrm{i}}}{\mathrm{J}_2(\mathbf{X}_{\mathrm{i}})} \quad , \quad \boldsymbol{\alpha}_{\mathrm{i}}(\mathrm{t=0}) = \mathbf{0} \qquad (8)$$

with c_i, d_i and m_i as material parameters defining the kinematic hardening and the static recovering, respectively.

The related hardening variables r and $\boldsymbol{\alpha}_{\mathrm{i}}$ are describing the degree of hardening, that corresponds in the material structure to the accumulation of immobile dislocations and that causes certain internal stresses k+R and $\mathbf{X}_{\mathrm{i}}$, respectively, at a certain temperature. All thermo-physical and material parameters are temperature-dependent and were determined for temperatures in the range of 470°C-590°C with 30°C temperature steps. A detailed description can be found by Sommitsch et al. (2006 b).

6. A LIFETIME RULE FOR COMPLEX PROCESSES

Cyclically loaded structures suffer a fatigue failure. Fatigue lifetime means in a macroscopic model the initiation of a macro-crack (typically a fraction of millimetre). Fatigue lifetime rules are usually formulated on the basis of mean quantities of a cycle, like stress or strain ranges (see, e.g., Chaboche and Gallerneau, (2001)). In contrast, time incremental lifetime rules (Majumdar and Maiya, (1980); Sermage et al., (2000)) evaluate the total damage in each time increment and, thus, can be applied also to complex multiaxial loading paths, for which the definition of a single loading parameter describing the entire cycle could be difficult. Furthermore, a time incremental lifetime rule can easily be implemented in a material sub-routine for finite element analysis of structures just as an evolution equation for an additional internal variable, the lifetime consumption D, $0 \le \mathrm{D} \le 1$. The following lifetime rule has been used:

$$\frac{\mathrm{dD}}{\mathrm{dt}} = \left(\frac{\sigma_{\mathrm{eq}}}{A}\right)^{m_l}\left(\frac{\dot{\mathrm{p}}}{\dot{\mathrm{p}}_0}\right)^{n_l}\dot{\mathrm{p}}_0 \,,$$

$$\sigma_{\mathrm{eq}} := \sqrt{\tfrac{3}{2}}\left\|\mathbf{S}\right\| \qquad (9),$$

where σ_{eq} is the Von Mises equivalent stress, $\dot{\mathrm{p}}$ the inelastic Mises equivalent strain-rate as defined in Eq. (6) and $\dot{\mathrm{p}}_0$ is a normalisation constant. The material parameters A and m_l describe the stress-dependence of the lifetime behaviour. An influence of the mean stress of a cycle was taken into account automatically by the fact that a stress process, which is non-symmetric to the zero-point in the stress space during a cycle, moves for the same stress range as in a symmetric process at higher stress magnitudes, nevertheless. The parameter n_l describes the time-dependence of the lifetime: for rate-independent behaviour n_l is equal to 1, n_l equal to zero means that a fully time-dependent lifetime behaviour is present. n_l was found to be positive but significantly lower than 1 for the investigated high temperature loading. The parameters A and m_l were determined from LCF tests with strain-rates of 10^{-3} s^{-1} and without hold-times. The parameter n_l was identified by the influence of hold-times in LCF tests on the lifetime behaviour. More details can be found by Sommitsch (2006 b). The cycles-to-failure $\mathrm{N_f}$ were calculated by the formula:

$$N_f \approx 1/(\Delta D)_s , \qquad (10)$$

where $(\Delta D)_s$ is the lifetime consumption within one saturated cycle. For the chosen extrusion examples, the simulations led to maximum lifetime consumption in the region of relatively high both temperature and equivalent stresses (figure 6a).

order to get both the temperature and radial stress boundary conditions for a subsequent cyclic simulation of the temperature and stress evolution in the container. Here, both the chosen constitutive model and the time incremental lifetime rule were coupled to the FEM model. Furthermore, the calculated tem-

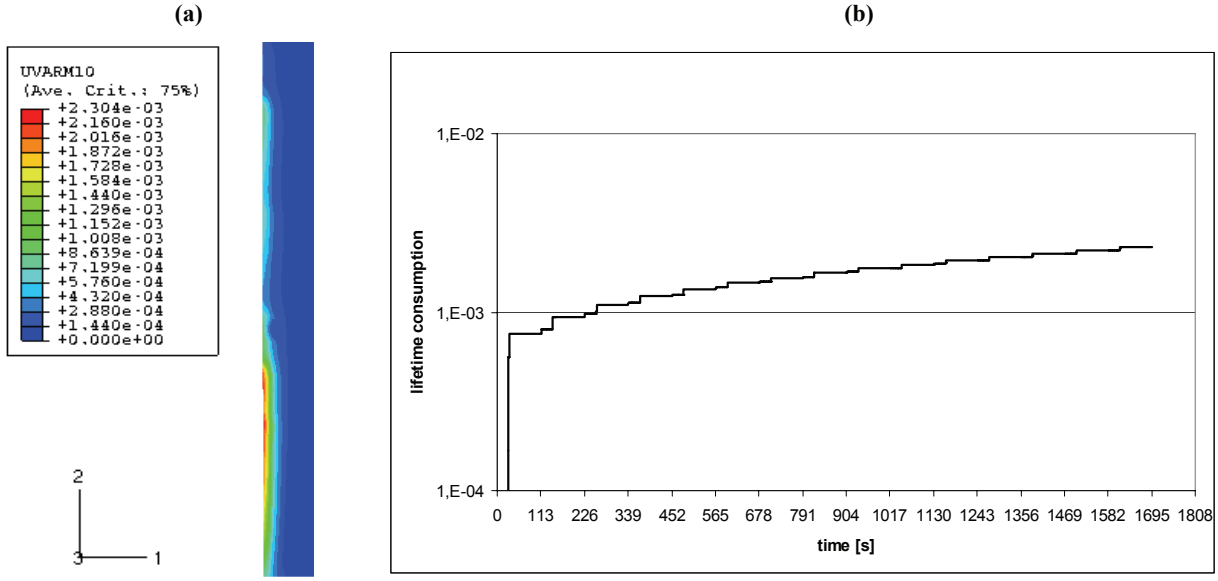

Fig. 6. *Resulting creep-fatigue damage (D) distribution at the region of maximum thermo-mechanical load at the inner wall of the liner (a). Lifetime consumption over 15 extrusion cycles for one selected element in the mostly damaged area of the liner (b).*

During extrusion, the equivalent stress and temperature maxima are not located at exactly the same place in the liner. However, the largest accumulated damage occurs in regions that exhibit maximum overlapping temperature and equivalent stress loading. Figure 6b depicts the lifetime consumption evolution with time for 15 extrusion cycles. For copper extrusion the calculated cycles-to-failure of the liner are 6,600. These results seem to be reasonable in comparison to real container lifetime.

7. CONCLUSIONS

A thermoviscoplastic constitutive model for the calculation of inelastic strains due to creep-fatigue loads in extrusion tools made of hot work steels was presented. Furthermore, a fatigue lifetime rule for complex multiaxial loading is proposed that is independent of single loading parameters to describe an entire cycle. Instead this lifetime rule evaluates the total damage in each time increment and, thus, can easily be implemented in a material sub-routine for finite element analysis of structures just as an evolution equation for an additional internal variable, the lifetime consumption. As an example, the lifetime of a liner during copper extrusion was predicted. Therefore the extrusion process was simulated in

perature and stress distribution was compared to measured values with the help of an extrusion test device.

REFERENCES

Chaboche, J.-L., 1993, Cyclic Viscoplastic Constitutive Equations, Part I: A Thermodynamically Consistent Formulation, *J. Appl. Mechanics*, 60, 813-821.

Chaboche, J.-L., Gallerneau, F., 2001, An Overview of the Damage Approach of Durability Modelling at Elevated Temperature, *Fatigue Fract. Engng. Mater. Struct.*, 24, 405-418.

Frenz, H., Meersmann, J., Ziebs, J., Kühn, H.-J., Sievert, R., Olschewski, J., 1997, High-Temperature Behaviour of IN 738 LC under Isothermal and Thermo-mechanical Cyclic Loading, *Mat. Sci. Eng.*, A 230, 49-57.

Krausz, A.S., Krausz, K., 1996, *Unified Constitutive Laws of Plastic Deformation*, Academic Press.

Krempl, E., 2001, Relaxation Behavior and Modeling, *Int. J. Plasticity*, 17, 1419-1436.

Lemaitre, J., Chaboche, J.-L., 1990, *Mechanics of Solid Materials*, Cambridge Univ. Press.

Majumdar, S., P.S. Maiya, P.S., 1980, A Mechanistic Model for Time-dependent Fatigue, *J. Eng. Mat. Techn.*, 102 , 159-167.

Olschewski, J., Sievert, R., Bertram, A., 1993, Non-isothermal Investigations on Ni-based Superalloys, Aspects of High Temperature Deformation and Fracture in Crystalline Materials, *Proc. JIMIS-7*, eds, Y. Hosoi et al., The Japan Institute of Metals, Nagoya, 641-648.

Sermage, J.P., Lemaitre, J., Desmorat, R., 2000, Multiaxial Creep-Fatigue under Anisothermal Conditions, *Fatigue Fract. Engng. Mater. Struct*., 23, 241-252.

Sommitsch, C., Wlanis, T., Hatzenbichler, T., Wieser ,V., 2006 a, Creep Fatigue in Extrusion Dies – Modelling and Simulation, *STEEL GRIPS*, 4, 51-55.

Sommitsch, C., Sievert, R., Wlanis, T., Günther, B., Wieser, V., 2006 b, Modelling of Creep-Fatigue in Containers during Aluminium and Copper Extrusion, *J. Comput. Mat. Sci*., in press.

Wieser, V., Sommitsch, C., Haberfellner, P., Lehofer, H., 2004, New Developments in the Design and Production of Container Assemblies, in: ET '04 – *Proc. 8th Inter. Aluminium Extrusion Technology Seminar*, Orlando, Vol. 1, 309-316.

PĘKNIĘCIE ZMĘCZENIOWE WIELOCZĘŚCIOWEGO POJEMNIKA PODCZAS WYCISKANIA NA GORĄCO – MODELOWANIE I DOŚWIADCZENIE.

Streszczenie

Artykuł przedstawia rozkład pól temperatur, naprężeń oraz zużycia materiału podczas trzech cykli wyciskania miedzi w dwuczęściowym pojemniku. Symulacja procesu obróbki cieplnej oraz ostateczny stan pojemnika zostały wykorzystane jako podstawa do opracowania kolejnych kroków zużycia materiału podczas cyklicznych etapów wyciskania. Symulacja numeryczna MES obejmuje modelowanie plastycznego wsadu i sztywnych narzędzi oraz kilku cykli tego samego procesu dla elastycznego pojemnika przy wykorzystaniu zależnych od czasu warunków brzegowych dla temperatury oraz nacisku. Powodem takiej procedury obliczeniowej jest krótszy czas symulacji niż w przypadku plastycznego procesu wyciskania. W celu weryfikacji obliczonych warunków brzegowych temperatury i nacisku na powierzchni styku, skonstruowano specjalną maszynę laboratoryjną do prowadzenia procesu wyciskania.

Submitted: September 24, 2006
Submitted in a revised form: December 4, 2006
Accepted: December 6, 2006